Small Submerged Vortex Generators for Turbulent Flow Separation Control

J. C. Lin* and F. G. Howard*
NASA Langley Research Center, Hampton, Virginia
and
G. V. Selby†
Old Dominion University, Norfolk, Virginia

The performance of low-profile submerged vortex generators for controlling moderate two-dimensional turbulent flow separation has been investigated experimentally. Surface static pressure measurements, as well as surface oil flow visualizations, have been used to explore the effect of these vortex generators on separation and reattachment locations and downstream pressure recovery. Drag measurements have also been used to evaluate the device (or parasitic) drag of these vortex generators. All of the vortex generators investigated have been shown to reduce the reattachment distance and increase pressure recovery. A small submerged (Wheeler-type) vortex generator with a device height of only 10% of the boundary-layer thickness is shown to perform as well as a conventional vane-type vortex generator with a device height (and device drag) an order-of-magnitude higher.

Nomenclature

C_p = pressure coefficient, $2(P-P_\infty)/\rho U_\infty^2$
h = height of vortex generator
ℓ = length of vortex generator
P = pressure
R_θ = Reynolds number based on momentum thickness
U = local velocity in the x direction
x,y = coordinates along and normal to the horizontal surface, respectively
α = vortex generator sweep angle
δ = boundary-layer thickness
θ = momentum thickness
λ = spanwise distance between each geometric cycle
ρ = density

Subscript
∞ = freestream value

Introduction

MOMENTUM or energy loss due to flow separation is detrimental to airfoil and diffuser performance and increases body drag. Excessive separation results in stalling, which can lead to catastrophic results. Controlling flow separation can result in an increase in system performance with consequent energy conservation, as well as weight and space savings. Thus, flow separation and its control is an important research area in fluids engineering.

A common flow separation control technique is to add momentum to the near-wall flow by redirection of higher momentum flow from the freestream region. Vortex generators have long been known to increase mixing between external streams and boundary layers.[1-10] Fluid particles with high momentum in the stream direction are swept along helical paths toward the surface to mix with, and to a certain extent replace, the retarded air at the surface. This air, in turn, is swept away from the surface. The vortices "energize" the low-energy boundary-layer flow through a three-dimensional process and delay separation in regions of high adverse pressure gradients. Although there are may kinds of vortex generators,[1] the vane-type generators introduced by Taylor[2] are the ones most often used. They consist of a row of small plates, or airfoils, that project normal to the surface and are set at an angle of incidence to the local flow to produce single trailing vortices. These vortex generators have been used in the past to produce attached flows and enhance aircraft wing lift.[3-7] They also have been used to avoid or delay separation in subsonic diffusers.[8,9] A more recent example is afterbody drag reduction on a C-130 aircraft using vortex generators.[10] However, all of these studies used vortex generators with device height h on the order of the boundary-layer thickness δ. Kuethe[11] has examined several wave-type submerged vortex generators with h/δ of 0.27 and 0.42 that were successful in reducing the intensity of sound generation in the wake region by suppressing the formation of the Kármán vortex street (implying a likely reduction in separation) and inducing a spanwise periodicity. A more recent study by Rao and Kariya[12] suggests that a concave slat-type submerged vortex generator with $h/\delta \sim 0.625$ may retain its effectiveness on a significantly reduced scale relative to the boundary-layer thickness. An in-depth study was recommended to identify optimum geometric parameters and to examine the parasitic drag.

The use of vortex "reinforcers" to augment vortex generator performance has also been suggested. An innovation in this area is the "Wheeler" vortex generator,[13,14] which consists of rows of triangular ramp-like devices shaped like overlapping (downstream-facing) arrowheads. In limited commercial trials in the trucking industry, up to 10% fuel mileage improvement for long-haul semitrailers was claimed. This type of vortex generator requires further study.

An objective of the current research is to experimentally investigate the relative performance of small submerged (Wheeler-type) vortex generators with respect to the conventional vane-type vortex generators, for controlling two-di-

Presented as Paper 89-0976 at the AIAA 2nd Shear Flow Control Conference, Tempe, AZ, March 13-16, 1989; received July 27, 1989; revision received Dec. 8, 1989.

*Aerospace Engineer, Viscous Flow Branch, Fluid Mechanics Division.

†Associate Professor, Mechanical Engineering and Mechanics Department. Senior Member AIAA.

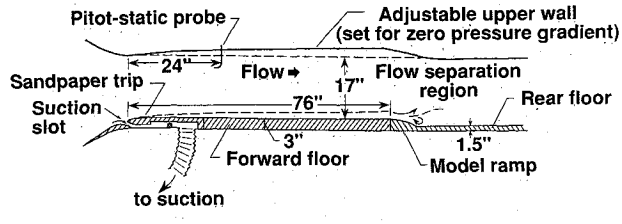

Fig. 1 Test configuration in tunnel.

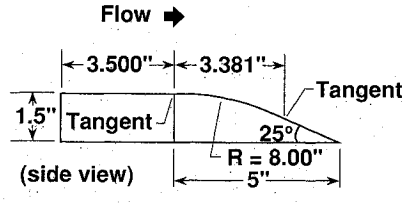

a)

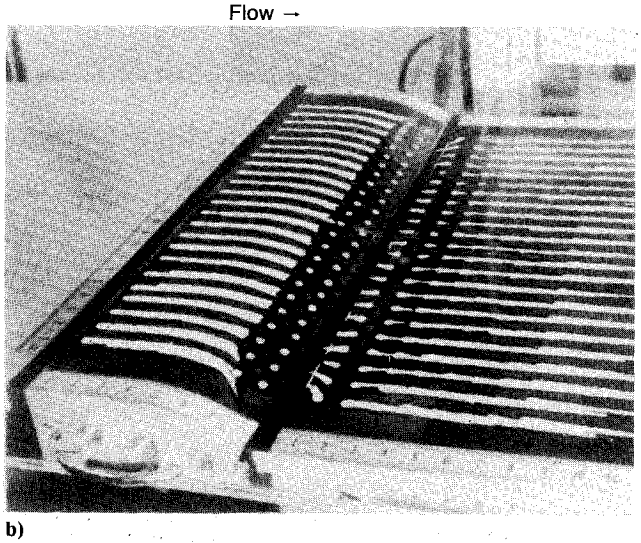

b)

Fig. 2 Reference model ramp: a) geometry of the model ramp; and b) oil flow visualization of the separation line.

mensional turbulent separated flow at low speeds. Surface pressure measurements, as well as flow visualization using surface oil dots, have been used to study the effect of these vortex generators on flow separation and reattachment. Drag-balance measurements have also been used to evaluate the device drag of these vortex generators.

Apparatus and Tests

Separation control experiments were conducted in the NASA Langley 20×28 in. Shear-Flow Control Tunnel. This is a low-turbulence subsonic open-circuit wind tunnel. In the current study, all of the experiments were conducted at a freestream speed of 132 ft/s. The freestream reference speed was measured by a pitot-static probe extended from the ceiling at the front of the test section.

Flow separation was established on a backward-facing curved ramp located approximately 76 in. from the test section entrance. See Fig. 1 for the test configuration. A suction slot at the test section entrance was used to remove the converging section boundary layer to eliminate any influence of upstream history on the test boundary layer. The new laminar boundary layer that developed downstream of the suction device was artificially tripped with a 2-in.-wide strip of sandpaper (36 grit). The ceiling height of the test section was adjusted to obtain zero pressure gradient along the test surface upstream of the ramp. The boundary layer just ahead of the separation ramp was fully turbulent and approximately 1.3 in. in thickness. At this same location, the spanwise momentum thickness θ variation across the test plate was within $\pm 2.5\%$ and the momentum thickness Reynolds number R_θ was approximately 9×10^3.

The baseline (or reference) separation model was a two-dimensional 25-deg ramp with a 8-in. shoulder radius, as shown in Fig. 2a. The width of the model was 28 in., which covered the entire test section in the spanwise direction. This model produced reasonably two-dimensional flow separation at approximately the midpoint of the ramp, or about 2δ downstream of the horizontal (or first) tangent point (see Fig. 2b).

The vortex generators investigated in the present study consisted of 1-in.-high (or $h/\delta \sim 0.8$) conventional vane-type (counter-rotating) and 1/2-in.-high and 1/8-in.-high ($h/\delta \sim 0.4$ and ~ 0.1, respectively) Wheeler-type devices. The geometry of these vortex generators is summarized in Fig. 3. All of the vortex generators were placed at varying distances upstream of the baseline separation.

Twenty-five static pressure orifices were located on the centerline of the separation ramp and 20 orifices were located on the centerline of the floor downstream of the ramp. The pressure orifices on the floor covered approximately two chord lengths of the ramp model. The pressure tubes for the orifices were connected to a motor driven valve that sequentially connected each orifice to a single differential pressure gage. All of the surface static pressure measurements were referenced to the freestream static pressure measurement located near the entrance of the test section. Because the flowfield downstream of the vortex generators was three-dimensional in nature, the spanwise pressure distribution measurements, over (at least) a device wavelength, were needed. This requirement was met by varying the location of the vortex generators in the spanwise direction.

The method of "oil dot" flow visualization, using a mixture of titanium dioxide and 10 cS silicone oil, was utilized to determine the surface flow patterns. Figure 2b indicates that this method worked quite well in identifying the separation line for the reference model. Oil dots were placed approximately 1 in. apart, in both the spanwise and flow directions, to obtain an overall flow pattern.

A small force balance was used to measure the device drag of all vortex generators in the current study. The drag balance was attached to a 4-×6-in. test surface with narrow gaps along all of its four sides and flush mounted on the tunnel floor upstream to the separation ramp. The balance test surface was supported by two vertical supports that were flexible in the flow direction but rigid in all other directions. A piezoresistive deflection sensor was used to convert the test surface displacement into a signal proportional to the drag force. The range of the drag balance was 0–1.3 lbf, with a resolution of 2.2×10^{-4} lbf. The vortex generator device drag measurements were conducted at two streamwise locations of 6 and 42 in. (or 5δ and 32δ, respectively) upstream of the separation ramp.

Results and Discussion

Flow visualization results for the vane-type vortex generator indicate that each pair of the 0.8δ-high counter-rotating vortex

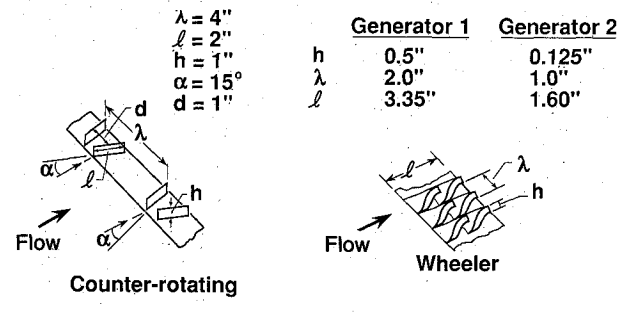

Fig. 3 Geometry of vortex generators.

generators provided mostly attached flow directly downstream (see Fig. 4). However, this attached flow was highly three-dimensional, and pockets of recirculating flow could be seen on the separation ramp between adjacent attached flow regions. Figure 4b shows that when the vortex generators were moved from 5δ to 15δ upstream of the baseline separation, the generators still maintained most of their effectiveness. Pressure distributions at three spanwise locations downstream of the counter-rotating vortex generators are presented in Fig. 5. The three spanwise locations are at a distance of 0, $\lambda/4$, and $\lambda/2$ away from the device centerline. The figure shows that, as expected, there are significant differences among the C_p distributions for various spanwise locations, which is another indication of a highly energized three-dimensional flow. When examining the baseline pressure distribution, it should be pointed out that the flow around a corner (or a shoulder) accelerates and decelerates symmetrically from the potential flow perspective, and this is the reason for the pressure drop along the upstream portion of the shoulder. Baseline separation occurred just before the sharply increasing C_p distribution began to level off, and reattachment occurred near the region of maximum C_p. The reattachment distance, therefore, was defined as the distance between the trailing edge of the model

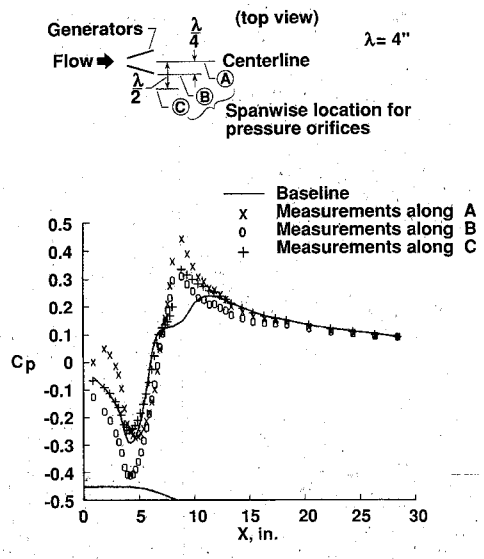

Fig. 5 Pressure distribution for 0.8δ-high counter-rotating vortex generators placed at 5δ upstream of baseline separation.

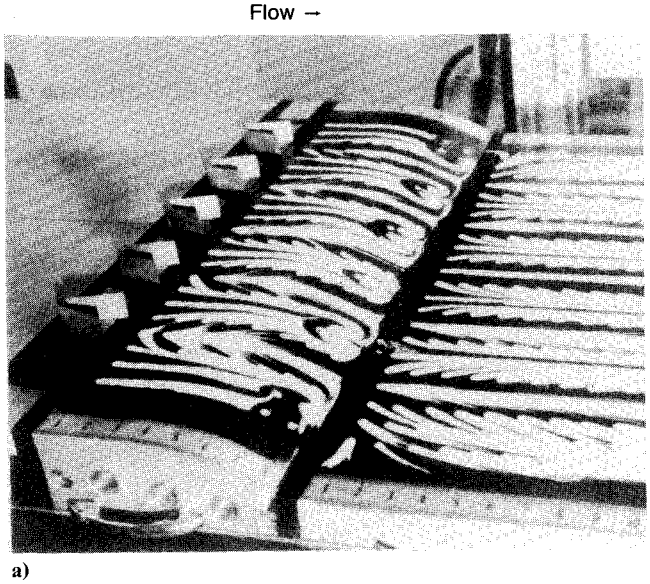

a)

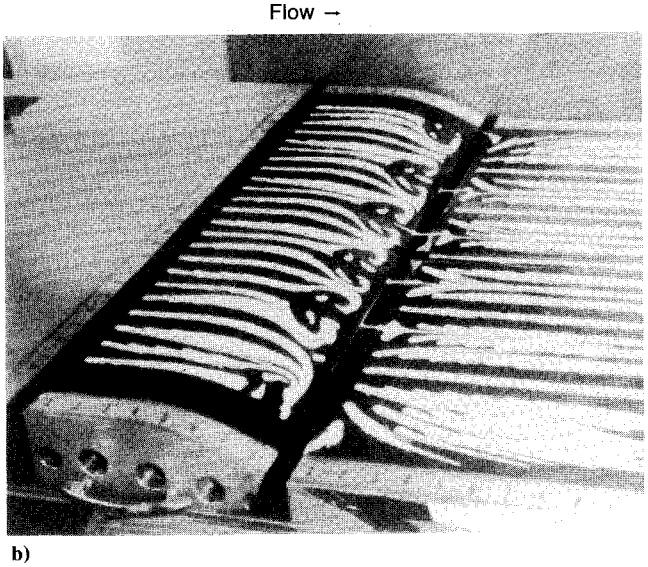

b)

Fig. 4 Oil flow visualization for 0.8δ-high counter-rotating vortex generators: a) generators at 5δ upstream of baseline separation; and b) generators at 15δ upstream of baseline separation.

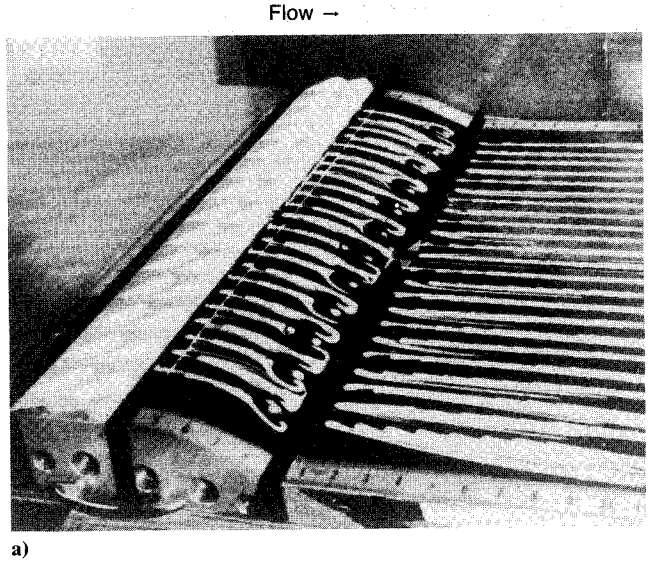

a)

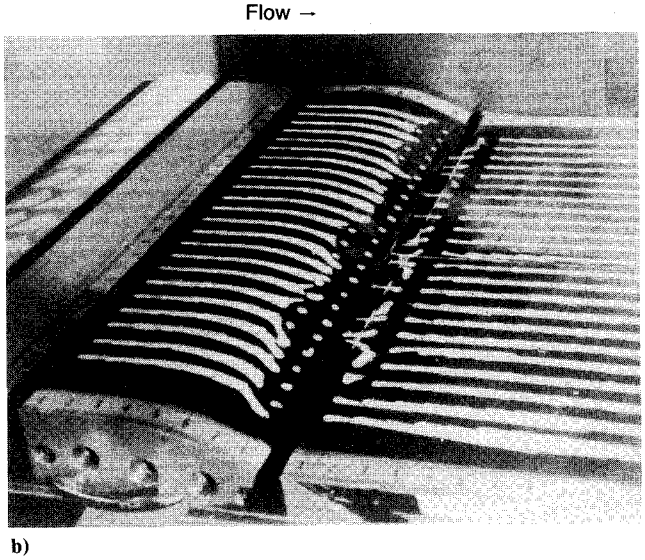

b)

Fig. 6 Oil flow visualization for 0.4δ-high Wheeler vortex generators: a) generators at 2δ upstream of baseline separation; and b) generators at 9δ upstream of baseline separation.

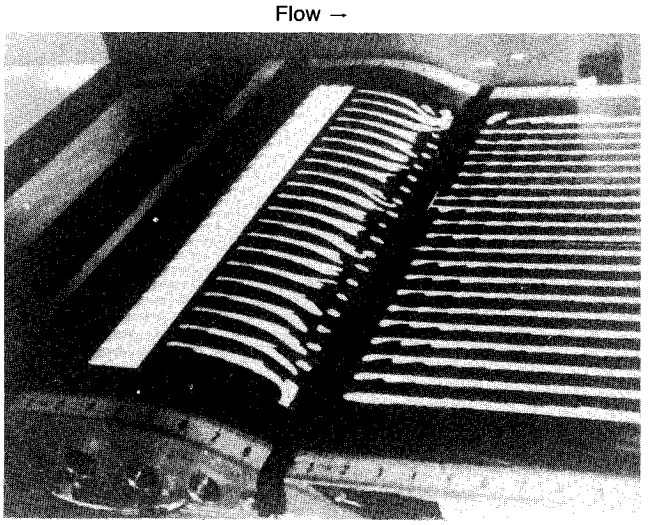

a)

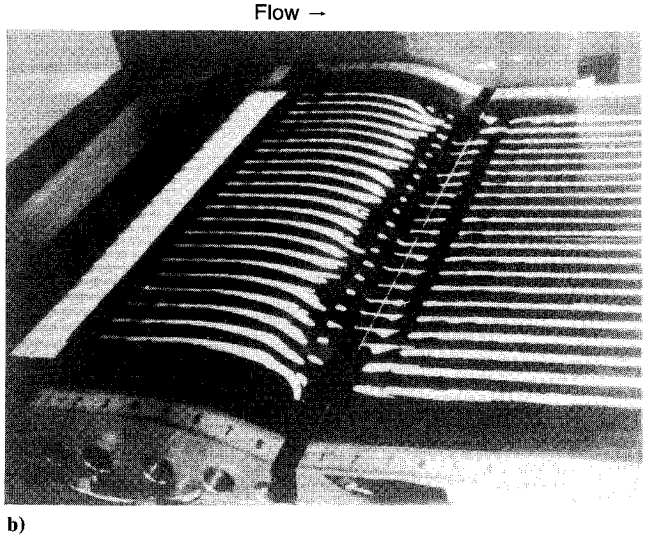

b)

Fig. 7 Oil flow visualization for 0.1δ-high Wheeler vortex generators: a) generators at 2δ upstream of baseline separation; and b) generators at 5δ upstream of baseline separation.

ramp and the streamwise location where the maximum C_p occurred. Figure 5 also indicates that the vane-type counter-rotating vortex generator can provide an improved pressure recovery; however, this vortex generator also reduced the pressure on the shoulder region of the ramp. This effect is desirable if one wants to increase lift, but results in a pressure drag penalty. The pressure reduction is due to an increase in local velocity resulting from the redirection of high momentum flow from the outer part of the boundary layer. This pressure reduction is probably also an indication that the vortices produced by the counter-rotating vortex generators were stronger than necessary. Weaker vortex generator would minimize the pressure reduction.

Flow visualization results for the Wheeler vortex generators indicate that the optimum streamwise location for these generators is just ahead of the horizontal tangent on the shoulder of the separation ramp (approximately 2δ upstream of the baseline separation). Figures 6a and 7a indicate that both the 0.4δ- and 0.1δ-high Wheeler vortex generators are quite effective in reducing the reattachment distance (up to 66%) over the baseline case, when installed at the optimum location. Although the 0.4δ-high Wheeler vortex generators provide some regions of partially attached flow, there are several well-organized pockets of recirculation at the base of the ramp. In addition, for this geometry, separation is delayed by approximately 0.5δ with respect to the baseline case. The 0.1δ-high Wheeler vortex generators also provide partially attached flow at the base of the ramp; however, the recirculation region is not as well organized and is less three-dimensional than in the 0.4δ-high case. Figure 6b shows that the effectiveness of the 0.4δ-high Wheeler vortex generators is less when the generators are moved to approximately 9δ upstream of the baseline separation. Figure 7b indicates that similar performance is displayed by the 0.1δ-high Wheeler vortex generators when placed approximately 5δ upstream of the baseline separation line. This reduction in downstream effective distance for the smaller Wheeler vortex generator suggests that the vortices produced were weak and dissipated quickly. Figure 8 presents the pres-

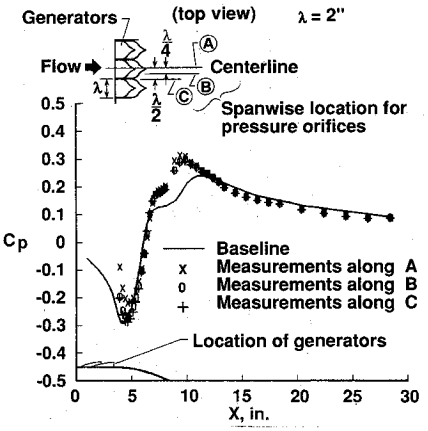

a)

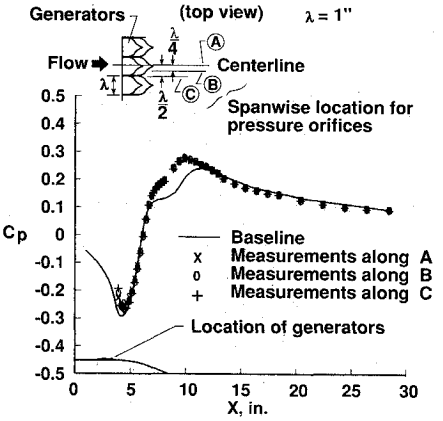

b)

Fig. 8 Pressure distribution for Wheeler vortex generators at 2δ upstream of baseline separation: a) 0.4δ-high Wheeler vortex generator; and b) 0.1δ-high Wheeler vortex generator.

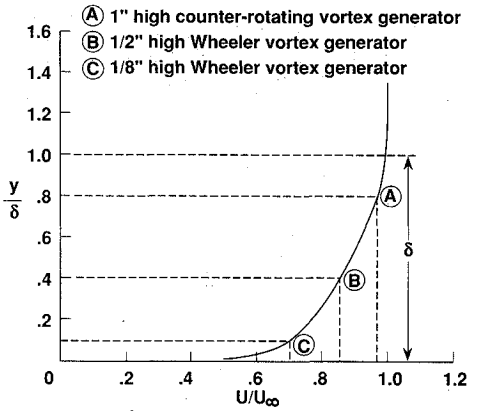

Fig. 9 Location of generator heights relative to the boundary-layer velocity profile.

sure distribution downstream of the Wheeler vortex generators with the generators in the optimum location (just ahead of the horizontal tangent). Figure 8a indicates that the 0.4δ-high Wheeler vortex generators produce a small spanwise C_p variation (reflecting the three-dimensional processes shown in the oil flow studies), which is much less than that associated with the 0.8δ-high counter-rotating vane-type vortex generators. The 0.1δ-high Wheeler vortex generators produced negligible spanwise C_p variations (Fig. 8b). This is another indication that the vortices are weak and produce less three-dimensional flow. In addition to the improved pressure recovery downstream of the ramp, the Wheeler vortex generators, unlike the vane-type counter-rotating vortex generators, also minimize the pressure reduction at the shoulder region of the ramp. This effect is especially prevalent with the 0.1δ-high generators and is beneficial to pressure-drag reduction.

The results from the 0.1δ-high Wheeler vortex generators become even more significant when it is noted that, in addition to the minimization of pressure reduction, this type of generator also incurs the least device-drag penalty. At a height of only about one-tenth of the boundary-layer thickness or $h/\delta \sim O$ (0.1), it performs almost as well as a vane-type generator with a device height on the order of δ. The individual device drag of the 0.1δ-high Wheeler vortex generator is only 6.3% percent of that of the 0.4δ-high Wheeler vortex generator and 2.3% of that of the 0.8δ-high vane-type counter-rotating vortex generator. Because the number of smaller Wheeler vortex generators must be increased to provide the same spanwise coverage as the larger generators, the installed device drag is approximately 13% of that for the 0.4δ-high Wheeler generator and 9% of that for the 0.8δ-high counter-rotating generator for equal spanwise coverage. Simplistically, the effectiveness of the smaller low-profile Wheeler vortex generator is at least partially due to the full velocity-profile characteristic of a turbulent boundary layer. Figure 9 shows the location of generator height relative to the boundary-layer velocity profile in the current study. Notice that even at a height of 0.1δ the local velocity is already 70% of the freestream value. Any further increase in height provides only a moderate increase in local velocity but dramatically increases generator drag. Low-profile vortex generators with h/δ of the order of 0.1 should be more closely examined for turbulent separation control, especially for applications where device drag is important.

Concluding Remarks

The relative performance of small submerged (Wheeler-type) vortex generators with respect to the conventional vane-type vortex generators was investigated experimentally for controlling moderate two-dimensional turbulent separated flow over a backward-facing ramp. Among the vortex generators investigated, the vane-type counter-rotating vortex generator with $h/\delta \sim 0.8$ provided the largest pressure recovery, but also imposed the largest device-drag penalty and further reduced the pressure in the shoulder region. Wheeler vortex generators reduced the reattachment distance by up to 66% with minimum pressure penalty in the shoulder region. The smaller Wheeler vortex generator with $h/\delta \sim 0.1$ (consequently, with much reduced device drag) performed as well as the larger Wheeler vortex generator with $h/\delta \sim 0.4$. The downstream effectiveness of the smaller Wheeler vortex generator was somewhat reduced, requiring placement no more than 2δ upstream of the baseline separation line.

Acknowledgments

The force balance was developed by Dr. Leonard M. Weinstein, Leader of the Turbulence Structure and Modeling Group, NASA Langley Research Center. The work of the third author was supported by the National Science Foundation under Grant MSM 8519116.

References

[1]Chang, P.K., *Control of Flow Separation*, Hemisphere, McGraw-Hill, New York, 1976, pp. 251-277.

[2]Taylor, H.D., "United Aircraft Research Department Summary Report on Vortex Generators," United Aircraft Corp. Research Dept., Rept. R-05280-9, March 7, 1950.

[3]Schubauer, G. B., and Spangenber, W. G., "Forced Mixing in Boundary Layers," *Journal of Fluid Mechanics,* Vol. 8, Part 1, May 1960, pp. 10-32.

[4]Pearcey, H. H., "Shock Induced Separation and Its Prevention by Design and Boundary Layer Control," *Boundary Layer and Flow Control*, Vol. 2, edited by G. V. Lachman, Pergamon, New York, 1961, pp. 1277-1312.

[5]Woolard, H. W., Benson, J. L., Stroud, J. F., and Drell, H., "Boundary-Layer Forced Mixing Investigation—Literature Survey and Progress Report," Lockheed-California Co., Rept. LR 18478, Burbank, CA, Nov. 1965.

[6]Fisher, J. W., "Flight Test Report—Use of Vortex Generators to Improve Performance of BLC Systems," Cessna Aircraft Co., Rept. No. 134-1, Wichita, KS, Dec. 23, 1954.

[7]Edwards, J. B. W., "Free Flight Tests of Vortex Generator Configurations at Transonic Speed," British Aeronautical Research Council, London, ARC Rept. No. 24662, Dec. 1962.

[8]Feir, J. B., "The Effects of an Arrangement of Vortex Generators Installed to Eliminate Wind Tunnel Diffuser Separation," Univ. of Toronto Institute of Aerospace Studies, Toronto, UTIAS No. 87, June 1965.

[9]Brown, A. C., Nawrocki, H. F., and Paley, P. N., "Subsonic Diffusers Designed Integrally with Vortex Generators," *Journal of Aircraft*, Vol. 5, No. 3, 1968, pp. 221-229.

[10]Calarese, W., Crisler, W. P., and Gustafson, G. L., "Afterbody Drag Reduction by Vortex Generators," AIAA Paper 85-0354, Jan. 1985.

[11]Kuethe, A. M., "Effect of Streamwise Vortices on Wake Properties Associated with Sound Generation," *Journal of Aircraft,* Vol. 9, No. 10, 1972, pp. 715-719.

[12]Rao, D. M., and Kariya, T. T., "Boundary-Layer Submerged Vortex Generators for Separation Control—An Exploratory Study," AIAA Paper 88-3546-CP, July 1988.

[13] Wheeler, G.O., "Means of Maintaining Attached Flow of a Flow Medium," U.S. Patent No. 4455045, U.S. Department of Commerce, Washington, DC, 1984.

[14]Lin, J. C., Howard, F. G., and Selby, G. V., "Turbulent Flow Separation Control Through Passive Techniques," AIAA Paper 89-0976, March 1989.

Walter B. Sturek
Associate Editor